TISSUE ENGINEERING: Part A
Volume 24, Numbers 1 and 2, 2018

DOI: 10.1089/ten.tea.2017.0035

termis
Tissue Engineering
& Regenerative Medicine
International Society

ORIGINAL ARTICLE

Near-Infrared Spectroscopy Predicts Compositional and Mechanical Properties of Hyaluronic Acid-Based Engineered Cartilage Constructs

Farzad Yousefi, MS,[1] Minwook Kim, PhD,[2,3] Syeda Yusra Nahri, BS,[1]
Robert L. Mauck, PhD,[2,3] and Nancy Pleshko, PhD[1]

Hyaluronic acid (HA) has been widely used for cartilage tissue engineering applications. However, the optimal time point to harvest HA-based engineered constructs for cartilage repair is still under investigation. In this study, we investigated the ability of a nondestructive modality, near-infrared spectroscopic (NIR) analysis, to predict compositional and mechanical properties of HA-based engineered cartilage constructs. NIR spectral data were collected from control, unseeded constructs, and twice per week by fiber optic from constructs seeded with chondrocytes during their development over an 8-week period. Constructs were harvested at 2, 4, 6, and 8 weeks, collagen and sulfated glycosaminoglycan content measured using biochemical assays, and the mechanical properties of the constructs evaluated using unconfined compression tests. NIR absorbances associated with the scaffold material, water, and engineered cartilage matrix, were identified. The NIR-determined matrix absorbance plateaued after 4 weeks of culture, which was in agreement with the biochemical assay results. Similarly, the mechanical properties of the constructs also plateaued at 4 weeks. A multivariate partial least square model based on NIR spectral input was developed to predict the moduli of the constructs, which resulted in a prediction error of 10% and R value of 0.88 for predicted versus actual values of dynamic modulus. Furthermore, the maximum increase in moduli was calculated from the first derivative of the curve fit of NIR-predicted and actual moduli values over time, and both occurred at $\sim$2 weeks. Collectively, these data suggest that NIR spectral data analysis could be an alternative to destructive biochemical and mechanical methods for evaluation of HA-based engineered cartilage construct properties.

Keywords: cartilage tissue engineering, hyaluronic acid, near-infrared spectroscopy, nondestructive modality, multivariate data analysis

Introduction

Articular cartilage covers bone surfaces in the diarthrodial joints and functions as a nearly frictionless tissue to dissipate high stresses generated by movement.[1] Cartilage consists primarily of proteoglycans and a collagen-rich matrix that is continuously remodeled by chondrocytes embedded within.[2] Because of its dense and avascular structure, cartilage has limited intrinsic healing capacity, once damaged as a result of disease and/or trauma. Clinical approaches such as microfracture, osteochondral autograft transfer, autologous chondrocyte implantation, and osteochondral allograft have been developed to address the limitations associated with the poor ability of articular cartilage to undergo self-repair.[3] These current clinical strategies for the treatment of articular cartilage injuries suffer from several limitations, including limited tissue regeneration, limited tissue availability for transplant/graft, tissue rejection by the host, and fibrocartilage development.[4–7]

To address these limitations, tissue engineering approaches have been studied comprehensively over the past two decades. Using a wide and combinational range of scaffolding materials, cell types, growth factors, culture conditions, and culture times, engineered tissues have been developed that possess compositional and biomechanical properties close to native tissue.[8–12] Nevertheless, clinical outcomes of repair with such tissues have been controversial.[13,14] It has also been shown that *in vitro* preculture of engineered implants and/or predifferentiation of mesenchymal stem cells could be beneficial for improved *in vivo* outcomes

[1]Tissue Imaging and Spectroscopy Lab, Department of Bioengineering, Temple University, Philadelphia, Pennsylvania.
Departments of [2]Orthopaedic Surgery and [3]Bioengineering, University of Pennsylvania, Philadelphia, Pennsylvania.

and functional cartilage repair.[15,16] Different strategies have been developed to improve maturation of precultured cartilage constructs.[8,17–19] A fundamental question for these approaches is, what degree of maturation should these engineered tissues reach before implantation?

The ability of engineered constructs to integrate with the native tissue is another determinant factor in the success of its future clinical application.[20] Marked stress concentrations at the boundaries of native tissue and the implant would be one consequence of failure in robust integration between two tissue types.[21] Therefore, both construct maturation and integration ability are key factors in the determination of optimum implantation time for *in vitro*-developed constructs. Recently, to estimate the appropriate implantation time for engineered cartilage constructs during *in vitro* culture, Fisher *et al.* introduced a trajectory-based tissue engineering approach and suggested a ''trade-off'' between functional maturation and integration,[22] where it was found that time-dependent changes strongly correlated with the capacity to develop an improved integration strength.

To implement a successful strategy based on construct maturation, it is necessary to assess the composition of developing engineered constructs *in vitro*. The destructive nature of gold standard methods for the determination of engineered construct composition, such as biochemical assays and histology, as well as the significant number of samples required for such assays, motivates the development of alternative nondestructive methods for construct evaluation. Current nondestructive alternatives for the characterization of engineered constructs during longitudinal development include magnetic resonance imaging (MRI),[23] X-ray imaging,[24] ultrasound imaging,[25] and optical imaging.[26] Over the past 10 years, much progress has been made in noninvasive magnetic resonance spectroscopy and MRI characterization of tissue-engineered cartilage.[27–36] As an example, Kotecha *et al.* characterized engineered cartilage using changes in T2-weighted MRI images and changes in magnetic resonance parameters such as water relaxation times.[28] In another study, Majumdar *et al.* used sodium MRI to assess the glycosaminoglycan (GAG) amount in stem cell chondrogenesis in a hybrid scaffold system.[30]

In another study, using ^{13}C NMR, Schulz *et al.* demonstrated the presence of chondroitin sulfate in cartilage tissue-engineered constructs.[35] Chondrogenesis of human marrow stromal cells (MSCs) seeded into chitosan/collagen type I scaffolds was studied by sodium NMR in another study.[29] Micro-MRI can yield micron size resolution (and better signal to noise compared to typical clinical imaging), but requires higher field strength, signal averaging, and/or powerful gradient sets, all of which may not be practical in a clinical setting.[37] Contrast-enhanced micro-CT is another option for nondestructive assessment of cartilage proteoglycan content.[38] However, this technique requires the addition of an external contrast agent, which may not be compatible with subsequent implantation of developing constructs.

Infrared (IR) spectroscopic methods for evaluation of tissues have been developed over the last two decades and have been utilized for different applications in various fields, including tissue engineering.[39,40] This technique is based on absorbance of IR light by tissue functional groups at specific vibrational frequencies, and thus, there is no need for external contrast agents.[39] Molecular vibrations generate absorption bands generally located in the mid-IR (MIR) range (between 400 and 4000 cm^{-1}) where they are the most intense and the simplest. Adjacent to the MIR, the near-IR (NIR) region covers the range between $\sim$4000 and 12,500 cm^{-1}. This region contains absorption bands corresponding to overtones and combinations of fundamental vibrations.[41] Spectroscopic modalities including imaging spectroscopy and fiber optic spectroscopy in both the MIR and NIR frequency regions can be used to evaluate tissue composition.[39,42] Fiber optic MIR spectroscopy is a nondestructive modality that can be used to evaluate tissue composition. Although this technique has been established as an approach to monitor cartilage degradation,[43] it is hampered by lack of sufficient penetration of photons into the sample, and hence information is obtained only from the surface (2–10 μm).[44] As articular cartilage as well as engineered cartilage constructs have a complex, heterogeneous structure,[45] it would be more desirable to apply a technique such as NIR spectroscopy, which has a greater depth of penetration than MIR spectroscopy and would permit sampling of the entire thickness of constructs up to $\sim$5 mm.[46–48] Although NIR spectroscopy offers more light penetration depth than MIR and does not require sample preparation, spectral signals obtained using NIR spectroscopy are not as specific as those obtained using MIR spectroscopy, and have not been fully investigated. In a recent study in our laboratory, the depth of penetration of NIR radiation into cartilage tissue was assessed using a fiber optic setup attached to an NIR spectrometer. It was found that the depth of penetration of the NIR radiation was dependent on the frequency (wavelength) of data acquisition and ranged from $\sim$1 to 2 mm in the 4000–5100 cm^{-1} range, to $\sim$3 mm in the 5100–7000 cm^{-1} range, and to $\sim$5 mm in the 7000–9000 cm^{-1} frequency range.[47]

In this study, we used a well-established and optimized scaffold in the field of cartilage tissue engineering. Among natural materials studied for cartilage tissue engineering, hyaluronic acid (HA) has been comprehensively studied and various parameters have been optimized to obtain superior culture protocols using this material.[8,9] HA is present in native adult articular cartilage and is involved in many cellular processes, including proliferation, morphogenesis, inflammation, and wound repair. HA hydrogels have been shown to support chondrocyte matrix deposition and chondrogenic differentiation of mesenchymal stem cells.[49]

In this study, a nondestructive NIR spectroscopic approach coupled with multivariate data analysis was developed for evaluation of engineered construct composition and maturation. We hypothesized that the NIR outcomes would correlate to gold standard compositional and mechanical outcomes related to the development of HA-based engineered cartilage constructs.

Materials and Methods

HA hydrogel synthesis

Methacrylated hyaluronic acid (MeHA) was synthesized as previously described.[50] Methacrylic anhydride (Sigma, $\sim$20-fold excess) was added to a solution of 1 wt% HA (Lifecore; molecular weight [MW] $\sim$ 64 kDa) in deionized water adjusted to a pH of 8 with 5 N NaOH (Aldrich) and reacted on ice for 24 h. For purification, the macromer solution was dialyzed (MW cutoff 5–8 kDa) against deionized

water for at least 48 h, and the final product was obtained by lyophilization. Lyophilized MeHA was sterilized by exposure to a biocidal UV lamp for 15 min. The macromer was dissolved to 1% (w/v) in sterile phosphate-buffered saline with 0.05% photoinitiator Irgacure-2959 (2-methyl-1-[4-(hydroxyethoxy)phenyl]-2-methyl-1-propanone) (Ciba-Geigy).

Chondrocyte isolation and three-dimensional culture

Articular cartilage was harvested from three juvenile bovine stifle joints (Research 87; Boylston). Tissues were digested in a spinner flask containing 250 U/mL type II collagenase (Worthington Biochemical), 99 mL DMEM (Life Technologies), 1 mL penicillin/streptomycin (10,000 U/mL penicillin and 10,000 μg/mL streptomycin; Life Technologies), and 0.2 mL fungizone (250 μg/mL amphotericin B and 205 μg/mL sodium deoxycholate; Life Technologies). Spinner flasks were incubated at 37°C and 5% CO_2 for 12 h. Chondrocytes were isolated from the digest solution by filtering through a 70-μm sterile nylon filter and centrifugation at 1000 *g*. The cell pellet was collected, reconstituted in 1× phosphate-buffered saline (Life Technologies), and cells were expanded through passage 3, combined, and encapsulated at 60,000,000 cells mL^{-1} in 1% (w/v) MeHA. Gels were polymerized by UV exposure (10 min) by a 365 nm Black-Ray UV lamp (Model #UVL-56) between glass plates separated by 2.25 mm spacers, and sterile 5 mm diameter punches (Miltex) were used to create chondrocyte-laden hydrogel cylinders.[51] Acellular MeHA hydrogels were also formed ($n=5$) for use as cell-free controls. Chondrocyte-laden hydrogel cylinders were placed in glass-bottomed six-well tissue culture plates (one scaffold per well) and were cultured in 5 mL of a chemically defined medium supplemented with TGF-b3 (10 ng mL^{-1}; R&D Systems) at 37°C and 5% CO_2. Culture media were replaced every 2–3 days. Glass-bottomed well plates (In Vitro Scientific) were used due to the absence of absorbance in the NIR spectral region. Cartilage constructs were harvested on day 0, 14 (2 weeks), 28 (4 weeks), 42 (6 weeks), and 56 (8 weeks) ($n=10$ per time point). Samples were weighed on each harvest day (wet weight) and thickness measured with a caliper. Constructs were then soaked in protease inhibitor (Sigma-Aldrich) and frozen at −20°C until biochemical analyses were performed.

NIR spectroscopy of acellular and cell-laden constructs

NIR spectra from acellular constructs (hydrogel only, $n=3$) were acquired in diffuse reflectance mode in the NIR range (8000–4000 cm^{-1}) at a spectral resolution of 16 cm^{-1} with a Perkin Elmer Spotlight 400 Imaging System (Perkin Elmer). A background spectrum of air was collected on a reflective aluminum surface, and sample spectra were collected from constructs placed on the same surface. Sample spectra were collected over time as the construct dehydrated ($t=0$, 15, 45, 265 min) for assessment of the contribution of water to the spectra and assignment of scaffold spectral absorbances.

Diffuse reflectance NIR spectra from cellular constructs were collected during each medium change (while the constructs were not immersed in culture media) using a Remspec NIR probe coupled to a Matrix-F spectrometer (Bruker Optics) using OPUS software v.5.5 (Bruker Optik GmbH). To maintain the sterility of the constructs during the data collection, the data collection process was done in a biological safety cabinet (BSC). The NIR probe was sprayed with 70% ethanol and placed on a stand in the BSC during data collection, and no contact was made between the constructs and the fiber optic tip. Background spectra of air were collected using a reflective mirror surface, and sample spectra were collected by positioning the probe 2 mm above the cartilage construct with the well plate placed on the mirrored surface. Each sample spectrum collected was the sum of 128 co-added scans across the spectral range of 10,000–4000 cm^{-1} with a spectral resolution of 16 cm^{-1}, and was ratioed to a background spectrum. Two NIR spectra were collected from each construct thrice per week over a period of 8 weeks.

NIR data preprocessing and multivariate data analysis (partial least squares)

NIR spectra were analyzed using Unscrambler X (CAMO Software). Two spectra per construct were averaged before data processing. Spectra were smoothed with a 51-point Savitzky–Golay algorithm and then preprocessed with an extended multiplicative scatter correction,[52] followed by area normalization and second derivative processing (to visualize peaks underlying the broad contours) with a 39-point Savitzky–Golay smoothing window.[53] Dynamic moduli of constructs were predicted using partial least square (PLS) regression with spectral data being X matrix and measured dynamic moduli being Y matrix. The PLS analysis approach finds linear combinations of the predictors (factors) to predict the response values. The number of factors for each model was determined by examining loading weights and comparison of the root mean square error of calibration (RMSEC) and root mean square error of cross-validation (RMSECV).[54] The quality of the model was evaluated based on the RMSEC or RMSECV (as a percentage of the range of data), and the R^2 of actual versus predicted values.

Biomechanical and biochemical analysis of chondrocyte-seeded constructs

Mechanical properties and biochemical composition were assessed for $n=6$ constructs per time point. All mechanical tests were performed on a custom-designed computer-controlled testing apparatus consisting of a stepper micrometer displacement actuator (Model 18515; Oriel Corp.), a Linear Variable Differential Transformer (Model HR100; Schaevitz) for measuring specimen deformation, and a load cell (Sensotec; range 622 N, 0.01 percent precision) for measuring the reaction force. The unconfined equilibrium compressive modulus was derived from a stress relaxation test (10% strain, 1000 s relaxation).[55] After equilibration, the dynamic modulus was determined using five sinusoidal cycles of compression at 1 Hz (1% strain amplitude).[56] After testing, each construct was weighed and digested in proteinase K (Sigma-Aldrich, P2308) before analysis for sulfated GAG (sGAG) and collagen content. sGAG content was analyzed using the 1,9-dimethylmethylene blue dye binding assay, and collagen using the chloramine-T based assay as previously described.[57,58]

Mathematical modeling of maturation (maximum rate of change)

Biomechanical and biochemical (GAG and collagen content) data and the related NIR spectral predictions of

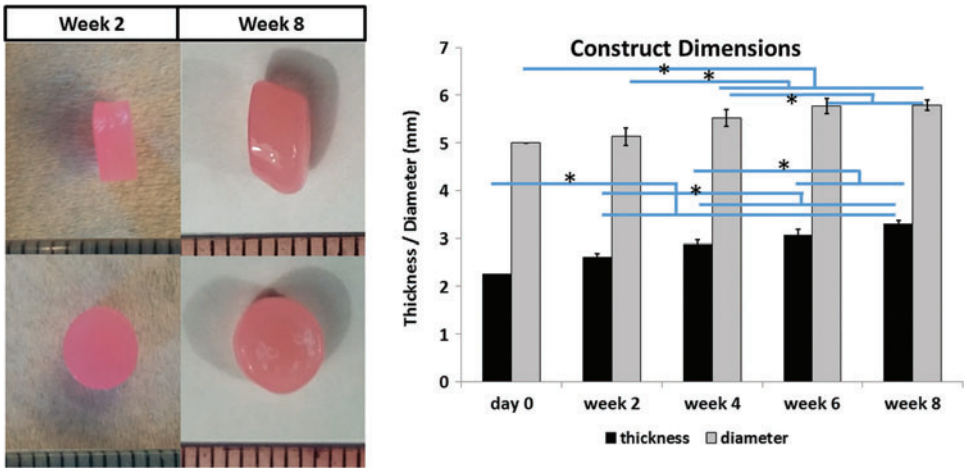

FIG. 1. Means and standard deviations of construct thickness and diameter ($n=6$ per time point, pictured on the *left*). Cartilage constructs were significantly thicker and larger in diameter compared to day 0 constructs for all time points. *Significant difference among values at different time points ($p<0.05$). Color images available online at www.liebertpub.com/tea

these data were plotted versus time. Data were fit individually with a sigmoidal curve ($y=a/(1+\exp(-(x-x0)/b))$) using SigmaPlot 12.0 (Sysstat Software). Using the determined parameters (a, $x0$, b), the first derivative of the function was calculated to determine where the maximum rate of change occurred in the original plots.

Statistical analysis

SigmaPlot 12.0 (Sysstat Software) was used to calculate average values and standard deviations, and for statistical analysis. Significant differences among different time points for each parameter were analyzed using ANOVA. *Post hoc* comparisons were performed with significance set at $p<0.05$. A Pearson correlation was performed to assess correlation of measured and predicted values from the PLS models, and between NIR-determined values and biochemical parameters.

Results

Engineered construct properties

The thickness and diameter of the engineered constructs increased by ~47% and 16%, respectively, after 8 weeks of culture (Fig. 1).

Collagen and sGAG content

Collagen content significantly increased from day 0 to week 4. After week 4, there were no significant differences in collagen content (Fig. 2a). The same trend was apparent in sGAG content (Fig. 2b). The amount of measured sGAG increased significantly during the first 4 weeks of culture, but no significant differences were observed after week 4 (Fig. 2b).

Mechanical properties

There was a fourfold increase in both equilibrium and dynamic moduli of the constructs from week 2 to 4. After week 4, there were no significant differences among the mechanical properties of the constructs (Fig. 3). As the trends were similar for both equilibrium and dynamic moduli, only the dynamic moduli will be discussed from this point forward.

NIR spectroscopy of acellular and cell-laden constructs

The contour of the NIR spectra of the acellular HA scaffolds changed as water was lost during air drying (Fig. 4a). The peaks that underlay the broad water peaks became more apparent as the HA dried over 5 h. Second derivative spectra were used to visualize the specific peaks

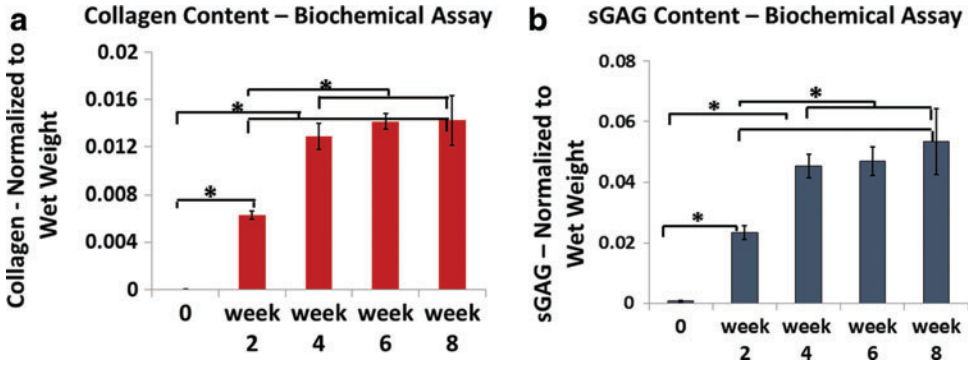

FIG. 2. Collagen **(a)** and sGAG **(b)** content (means and standard deviations) assessed by biochemical assay of harvested constructs ($n=6$ per time point). Construct collagen and sGAG content generally increased through 4 weeks in culture, but not after that. *Significant difference among values at different time points ($p<0.05$). sGAG, sulfated glycosaminoglycan. Color images available online at www.liebertpub.com/tea

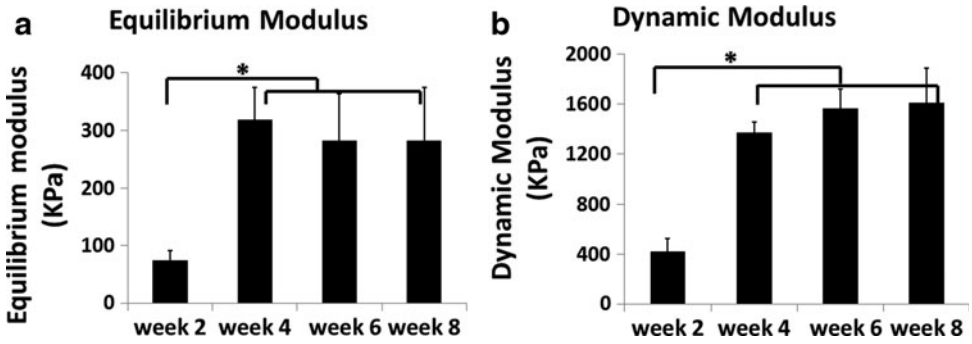

FIG. 3. Equilibrium **(a)** and dynamic **(b)** moduli were assessed using an unconfined compression test, with means and standard deviations presented for $n=6$ constructs per time point. Both moduli increased significantly from week 2 to 4, but no significant change was observed after week 4. *Significant difference among values at different time points ($p<0.05$).

that underlie the broad bands in the raw NIR spectra (Fig. 4b). The water peak at $\sim$5334 cm^{-1} was observed to shift to 5210 cm^{-1} after 265 min of drying. Another water peak at 7135 cm^{-1} shifted to 7086 cm^{-1} after 15 min, and then disappeared after 45 min of drying (Fig. 4b). The peaks that remained in the combination and first overtone regions (4000–4500 cm^{-1} and 5500–6000 cm^{-1}, respectively) were attributed to absorbances from C-H stretch combinations and overtones from the hydrogel.

The NIR spectra of cell-laden constructs were dominated by peaks associated with water molecule vibrations at $\sim$7135 (first overtone of the OH-stretching band), 5300 (combination of the OH-stretching band and the O-H bending band) and 8643 cm^{-1} (the combination of the first overtone of the O–H stretching and the OH-bending band)[59] (Fig. 5a). In the cell-seeded constructs, the only peak that was not present in the day 0 spectrum, but was clearly present in all other spectra, was the peak centered at 4443 cm^{-1}. This peak arises from the combination band of the C-H stretch and C-H deformation of peptide bonds,[60] and thus is a marker of chondrocyte matrix formation. NIR-determined matrix formation, based on the intensity of this peak, mirrored the sGAG and collagen found in the constructs (Fig. 6a–c), where both biochemically and spectroscopically derived values increased up to the week 4 time point and plateaued afterward.

Construct maturation

The development of the construct properties, including collagen, and sGAG content increase were modeled very well with a sigmoidal curve fit, with R values >0.87 for all

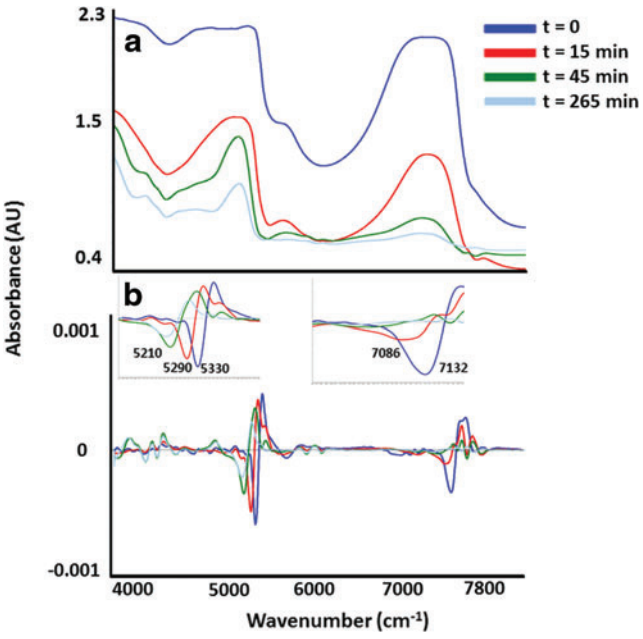

FIG. 4. NIR raw spectra **(a)** and second derivative spectra **(b)** of acellular HA constructs. As water evaporated from the constructs over time, absorbances from the HA molecule became visible in both raw and second derivative spectra. The zero time point refers to the initial data collection time immediately after removing the acellular construct from PBS, and the next data collections were performed after 15, 45, and 265 min. HA, hyaluronic acid. Color images available online at www.liebertpub.com/tea

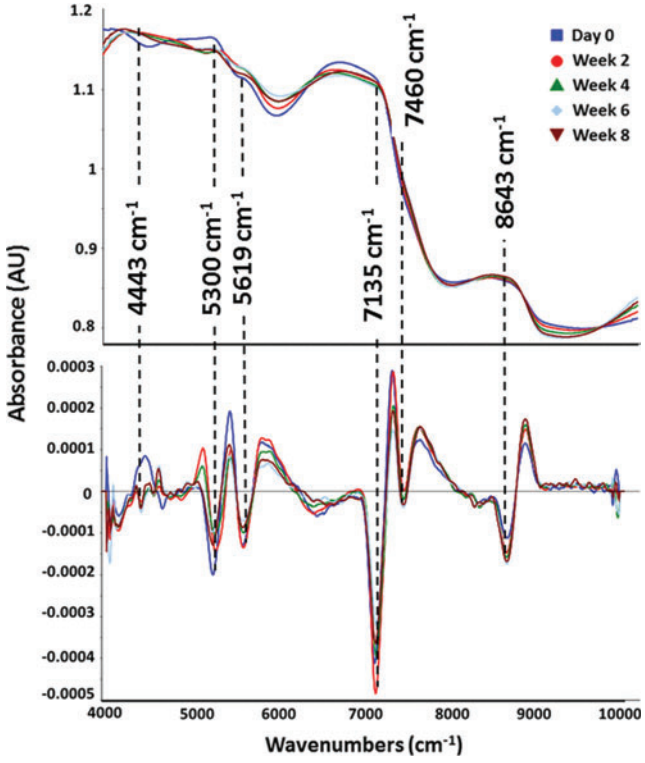

FIG. 5. NIR raw spectra **(a)** and second derivative spectra **(b)** of engineered cartilage constructs showing the water absorbance domination. Spectral details are resolved using second derivative spectra, and peaks reflecting specific matrix and water components are noted with *dashed lines*. Color images available online at www.liebertpub.com/tea

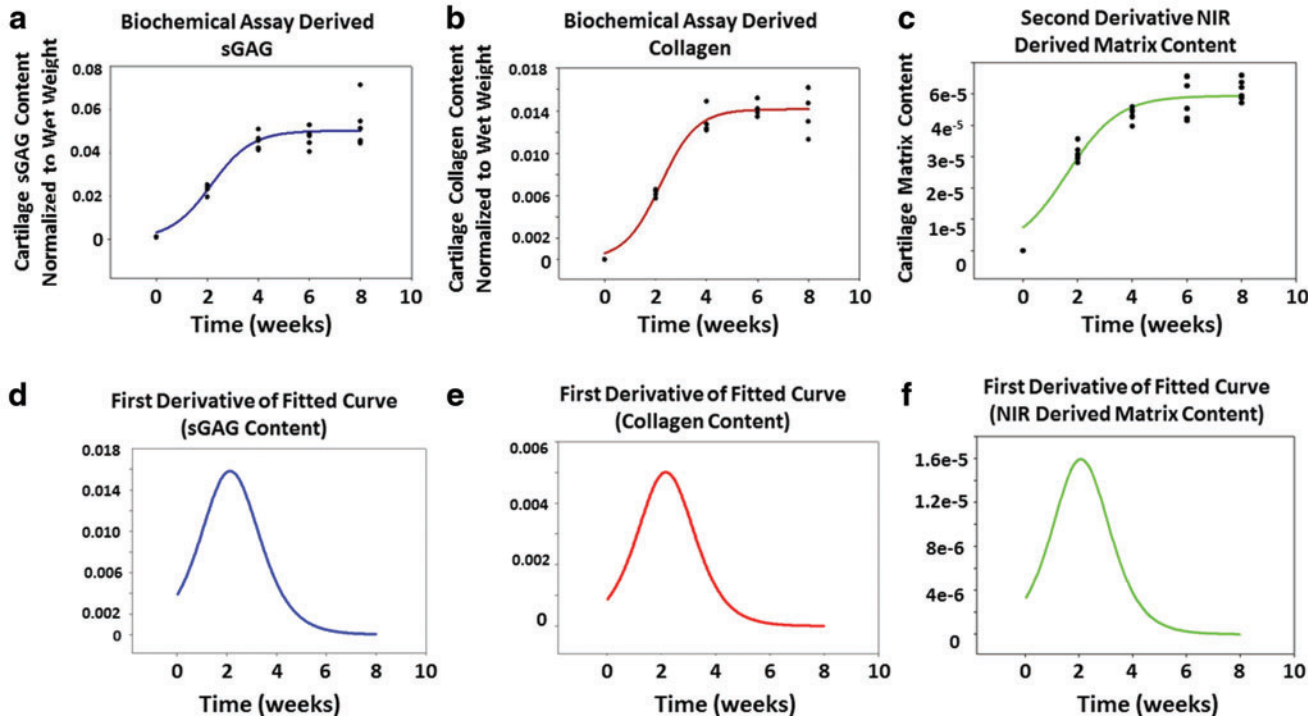

FIG. 6. Sigmoidal curve fits of **(a)** sGAG, **(b)** collagen, and **(c)** NIR-derived cartilage matrix data suggest a similar trend in longitudinal development. First derivatives of fitted curves for **(d)** sGAG, **(e)** collagen, and **(f)** NIR-derived cartilage matrix suggest that the maximum rate of construct maturation occurs at week 2, 2.1, and 2.2, respectively. Color images available online at www.liebertpub.com/tea

parameters (Fig. 6a–c). These data showed that the compositional parameters plateaued at week 4, which indicates no significant change was observed in the measured values after this time point. The maturation rate, as determined by the first derivative analysis of fit curves, revealed that week 2 was the time at which the maximum maturation rate occurred for compositional parameters, as well as for the NIR-derived matrix content (Fig. 6d–f). Interestingly, the trend in the dynamic moduli of the constructs and in compositional development is in reasonable agreement with the biochemical assay results (Fig. 7a). The maximum rate of increase in mechanical properties occurring at ~week 2 is very close to the time point for the maximum rate of change in sGAG and collagen content, as well as the maximum rate of change in cartilage matrix predicted by the NIR spectra (Fig. 7c).

Prediction of biochemical and mechanical properties with NIR spectral data

NIR spectral data PLS predictions of biochemical composition and dynamic moduli of the constructs resulted in errors of 10–11% of the parameter range for the calibration and validation of the models, and resulted in significant correlations to the experimental values (Table 1 and Fig. 7a, b). The first derivative plots revealed that the maximum time point for rate of change for both measured and PLS-predicted moduli data occurred at ~week 2 (Fig. 7c, d).

Discussion

Successful tissue engineering approaches require integration of implanted engineered constructs with surrounding host tissue to maintain the overall integrity and long-term functionality of the restored tissue, in particular when it is exposed to external loads. The concept of determination of optimal implantation time by choosing the time point at which maximum development rate occurs, rather than maximum maturation state, was recently formulized as ''trajectory-based'' tissue engineering by Fisher *et al.*[22] There, it was concluded that a strong correlation exists between maturation rate of engineered constructs and their integration capacity. This conclusion was in agreement with a previous study by another group.[61] In this study, we developed a nondestructive spectroscopic approach for assessment of chondrocyte-seeded HA hydrogel construct composition during *in vitro* development. With these data, which also correlate with mechanical properties of the constructs, it is possible to identify the time point at which maximum construct maturation rate occurs, and hence the optimum time point for implantation. Recently, the potential for improvement in matrix properties of engineered cartilage tissue has been investigated using physiologic loading in bioreactor systems,[62] as well as sequential supplementation with TGF-b3 growth factors.[63] The results of these studies demonstrate that any change in the mechanical and biochemical treatment of engineered tissue could lead to different properties of constructs at different time points, and it is likely that NIR spectroscopy could be used to assess those differences nondestructively.

For the application of nondestructive NIR to HA constructs, a critical step was gaining insight into the spectral features in the NIR spectrum of HA, which had not previously been investigated. NIR spectra of acellular HA

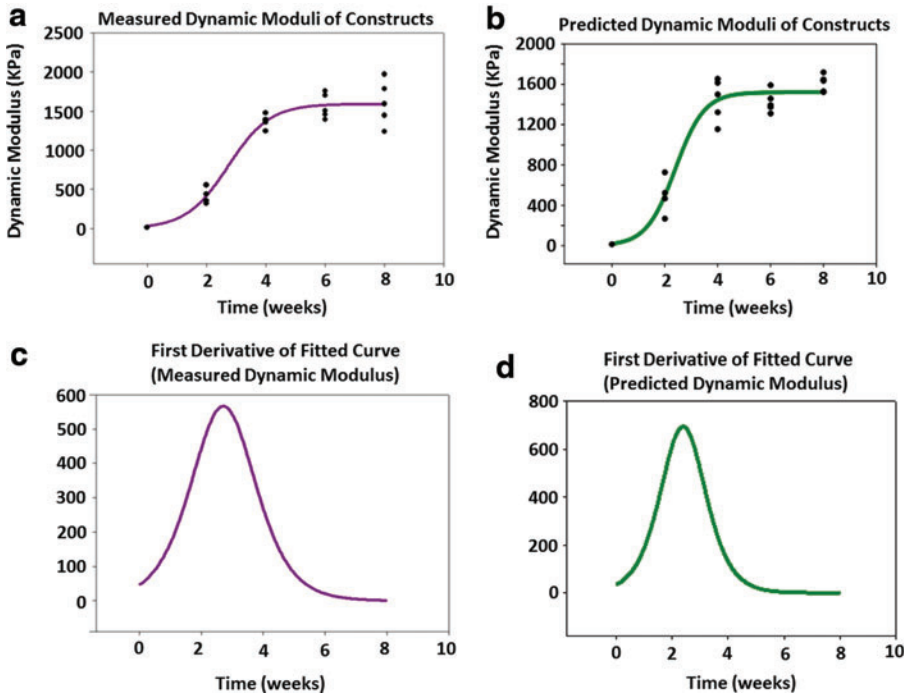

FIG. 7. Sigmoidal curve fits of **(a)** experimentally measured dynamic modulus and **(b)** dynamic modulus predicted by a partial least square analysis of NIR spectral data. Equilibrium moduli data are similar (not shown). The first derivative of the fitted experimental curve **(c)** and predicted curve **(d)** suggest that the maximum change in mechanical properties occurs at week 2.1 and 2.3, respectively. Color images available online at www.liebertpub.com/tea

constructs were evaluated to assign IR absorbance peaks to scaffolding material in the absence of cells and cell-associated matrix contributions to spectra. NIR spectra are very sensitive to the contributions of water, and these spectra were dominated by water in two regions, 5000–5300 cm^{-1}, the combination region, and 7000–7200 cm^{-1}, the first overtone region. Using a water evaporation technique, however, it was possible to visualize the absorbance bands that underlie the strong water peaks. Although it was not investigated in this study, it is possible that changes in the water absorbance frequencies and relative intensities with tissue growth could yield insight into the quality of the matrix formed.

In this study, we developed engineered HA-based cartilage constructs and demonstrated that both mechanical and compositional properties followed a sigmoidal maturation curve similar to that reported in previous studies.[22] The plateau time for chondrocyte-laden constructs are different from MSC-laden constructs; the former plateaus at week 4, whereas the latter plateaus at week 9. This difference could be explained by cell–hydrogel interactions, which would modulate the rate and extent of functional chondrogenesis as well as time (first 7–10 days) required for MSCs to differentiate toward a chondrocyte-like phenotype and initiate matrix production. Depending on culture conditions, cell type, and scaffold material, the plateau time could change.[18] Results of spectrally collected data from the constructs suggest a great similarity to biochemical and mechanical data in terms of the trajectory maturation curve. Changes in construct size were also consistent with observations in previous studies.[64,65]

Table 1. Partial Least Square Model Predictions of Mechanical and Compositional Parameters Based on NIR Spectral Data

	Model error (%)	*Correlation (R)*	p
Dynamic modulus prediction	10	0.88	<0.0001
Collagen content prediction	11	0.94	<0.0001
sGAG content prediction	10	0.94	<0.0001

sGAG, sulfated glycosaminoglycan.

It is still not confirmed whether the optimal time for construct implantation should be based on composition or mechanical properties. Miot *et al.* used histological and histomorphometric analysis to determine the maturation stage of constructs. They used collagen type II/I ratio as the indicator of maturity in constructs, which were undergoing *in vitro* culture and, together with histological and biochemical analysis, concluded that 2-week precultured constructs obtained the best score among all constructs (cell free, 2-day, 2-week, or 6-week precultured constructs) in a goat model study.[66] Hunter *et al.* measured the native/engineered tissue interface strength by a push-out test in three different scaffolds, including agarose, fibrin, and polyglycolic acid, at two different time points (day 20 and 40). They concluded that tissue–tissue adhesion potential was not significantly different for two studied time points. They proposed that using relatively mature tissues for implantation rather than immature ones would result in better *in vivo* outcomes.[61] Vinardell *et al.* performed a comparison of chondrocyte- and MSC-laden agarose constructs and compared the integration of two constructs laden with different cell types by a push-out test. They concluded that the higher failure stress in push-out test for chondrocyte-laden cells compared to MSC-laden constructs may be a result of higher GAG content, which results in greater swelling of the engineered construct in the defect site. Although they did not study different time points, their results still suggested that there is a correlation between biochemical content and

integration potential of engineered constructs.[67] In another study by Obradovic *et al.*, authors studied integrative properties of constructs by evaluation of tissue remodeling and adhesive strength patterns in an *in vitro* study and concluded that less-mature constructs obtained higher integrative properties compared to more mature constructs.[68] In light of all these relatively contradictory results, as well as the recent study by Fisher *et al.*,[22] we believe that less-mature, but rapidly developing constructs may need to be selected for implantation to obtain better *in vivo* outcomes. As shown in this study, to select the time point in which the maximum development rate occurred through biochemical and mechanical analyses, a considerable number of constructs ($n = 50$) were required for an 8-week study. Based on the results of our proposed NIR method, the maximum development rate time point occurred at the same time point as was identified by destructive biochemical and mechanical methods. Therefore, our data support that nondestructive NIR spectroscopy analysis could be utilized to find the optimum implantation time with a minimal number of samples. This is based on the fact that the NIR spectroscopy modality is nondestructive and data could be collected from constructs frequently without the need to sacrifice them.

Use of other techniques for nondestructive analysis of cartilage, including NIR for assessment of cartilage quality, has also been performed.[42,69–74] For example, Afara *et al.* evaluated the potential of NIR spectroscopy for quantifying tissue alterations in osteoarthritis animal models. Mankin grade, histology, and loss of tissue matrix, measured by the cartilage thickness, were found to correlate significantly with the NIR absorption spectra.[70] In another study, Spahn *et al.* reported the possibility of implementing NIR spectral assessment for identification of low-grade lesions during routine arthroscopy.[74] In a different study by the same group, it was shown that NIR spectral data had a better interobserver correlation in comparison with a routine subjective grading method in an arthroscopic evaluation of cartilage defects.[73] Also, from our laboratory, McGoverin *et al.* showed that NIR spectral data collected from human tibial plateaus correlated with histologic Mankin score.[75] With respect to engineered tissue evaluation, nondestructive NIR-based tissue-engineered construct development was recently carried out by our group for the assessment of polyglycolic acid-based scaffolds.[40,72] In those studies, an NIR absorbance specific to polyglycolic acid was used to monitor degradation of the scaffold. In a different study, ultrasound was used as a nondestructive measurement to evaluate the evolution of neo-tissue formation within a synthetic hydrogel.[76] Mansour *et al.* and Trachtenberg *et al.* have recently reviewed a comprehensive list of nondestructive evaluation methods used for cartilage and engineered cartilage tissue.[37,77] Kunstar *et al.* used Raman microspectroscopy to study ECM production of primary bovine chondrocytes seeded onto three-dimensional scaffolds and assigned two peaks (937 and 1062 cm^{-1}) to collagen and proteoglycan, respectively.[78]

Although these data are encouraging, there are several challenges in implementing NIR spectral data collection from engineered constructs. An important consideration is the potentially large effect of water on NIR spectra, which could obscure important matrix peaks. However, investigation of second derivative spectra and use of multivariate analyses are approaches to overcome this issue. Another consideration is that during NIR data collection, media need to be removed from the wells to minimize the interference of external water. Although the time for NIR data collection ranges from 3 to 6 min per construct, depending on the number of scans as well as spectral resolution and other factors, this short period of time that constructs are being exposed to air could still affect the encapsulated cells and cause oxidative stress.[79] Use of a chamber with well-controlled temperature/humidity and CO_2 level during NIR data collection could help to address this issue, and is under consideration.

Collectively, these data suggest that NIR spectroscopy could be used nondestructively to monitor the development of HA-based engineered cartilage tissue. As the appropriate time to harvest engineered tissues for implantation is critical to obtain optimum clinical results, NIR spectroscopy could be a potential technique to predict implantation time for HA-based, and other, engineered cartilage constructs.

Acknowledgment

This work was supported by NIH R01AR056145 (N.P.) and R01 EB008722 (R.L.M.).

Disclosure Statement

No competing financial interest exists.

References

1. Ateshian, G.A., and Hung, C.T. Patellofemoral joint biomechanics and tissue engineering. Clin Orthop Relat Res **436,** 81, 2005.
2. Guilak, F., and Hung, C.T. Physical regulation of cartilage metabolism. Basic Orthop Biomech Mechanobiol **3,** 179, 2005.
3. Cokelaere, S., Malda, J., and van Weeren, R. Cartilage defect repair in horses: current strategies and recent developments in regenerative medicine of the equine joint with emphasis on the surgical approach. Vet J **214,** 61, 2016.
4. Basad, E., Ishaque, B., Bachmann, G., Sturz, H., and Steinmeyer, J. Matrix-induced autologous chondrocyte implantation versus microfracture in the treatment of cartilage defects of the knee: a 2-year randomised study. Knee Surg Sports Traumatol Arthrosc **18,** 519, 2010.
5. Chahal, J., Gross, A.E., Gross, C., Mall, N., Dwyer, T., Chahal, A., Whelan, D.B., and Cole, B.J. Outcomes of osteochondral allograft transplantation in the knee. Arthroscopy **29,** 575, 2013.
6. Knutsen, G., Drogset, J.O., Engebretsen, L., Grontvedt, T., Isaksen, V., Ludvigsen, T.C., Roberts, S., Solheim, E., Strand, T., and Johansen, O. A randomized trial comparing autologous chondrocyte implantation with microfracture. J Bone Joint Surg Am Vol **89A,** 2105, 2007.
7. Revell, C.M., and Athanasiou, K.A. Success rates and immunologic responses of autogenic, allogenic, and xenogenic treatments to repair articular cartilage defects. Tissue Eng Part B Rev **15,** 1, 2009.
8. Erickson, I.E., Kestle, S.R., Zellars, K.H., Dodge, G.R., Burdick, J.A., and Mauck, R.L. Improved cartilage repair via in vitro pre-maturation of MSC-seeded hyaluronic acid hydrogels. Biomed Mater **7,** 10, 2012.
9. Erickson, I.E., Kestle, S.R., Zellars, K.H., Farrell, M.J., Kim, M., Burdick, J.A., and Mauck, R.L. High mesenchyrnal stem

cell seeding densities in hyaluronic acid hydrogels produce engineered cartilage with native tissue properties. Acta Biomater **8,** 3027, 2012.
10. Gooch, K.J., Blunk, T., Courter, D.L., Sieminski, A.L., Bursac, P.M., Vunjak-Novakovic, G., and Freed, L.E. IGF-I and mechanical environment interact to modulate engineered cartilage development. Biochem Biophys Res Commun **286,** 909, 2001.
11. Lima, E.G., Bian, L., Ng, K.W., Mauck, R.L., Byers, B.A., Tuan, R.S., Ateshian, G.A., and Hung, C.T. The beneficial effect of delayed compressive loading on tissue-engineered cartilage constructs cultured with TGF-beta 3. Osteoarthritis Cartilage **15,** 1025, 2007.
12. Ng, K.W., O'Conor, C.J., Kugler, L.E., Cook, J.L., Ateshian, G.A., and Hung, C.T. Transient supplementation of anabolic growth factors rapidly stimulates matrix synthesis in engineered cartilage. Ann Biomed Eng **39,** 2491, 2011.
13. Ando, W., Fujie, H., Moriguchi, Y., Nansai, R., Shimomura, K., Hart, D.A., Yoshikawa, H., and Nakamura, N. Detection of abnormalities in the superficial zone of cartilage repaired using a tissue engineered construct derived from synovial stem cells. Eur Cells Mater **24,** 292, 2012.
14. Adachi, N., Ochi, M., Deie, M., Nakamae, A., Kamei, G., Uchio, Y., and Iwasa, J. Implantation of tissue-engineered cartilage-like tissue for the treatment for full-thickness cartilage defects of the knee. Knee Surg Sports Traumatol Arthrosc **22,** 1241, 2014.
15. Marquass, B., Schulz, R., Hepp, P., Zscharnack, M., Aigner, T., Schmidt, S., Stein, F., Richter, R., Osterhoff, G., Aust, G., Josten, C., and Bader, A. Matrix-associated implantation of predifferentiated mesenchymal stem cells versus articular chondrocytes in vivo results of cartilage repair after 1 year. Am J Sports Med **39,** 1401, 2011.
16. Steck, E., Fischer, J., Lorenz, H., Gotterbarm, T., Jung, M., and Richter, W. Mesenchymal stem cell differentiation in an experimental cartilage defect: restriction of hypertrophy to bone-close neocartilage. Stem Cells Dev **18,** 969, 2009.
17. Byers, B.A., Mauck, R.L., Chiang, I.E., and Tuan, R.S. Transient exposure to transforming growth factor beta 3 under serum-free conditions enhances the biomechanical and biochemical maturation of tissue-engineered cartilage. Tissue Eng Part A **14,** 1821, 2008.
18. Erickson, I.E., Huang, A.H., Chung, C., Li, R.T., Burdick, J.A., and Mauck, R.L. Differential maturation and structure-function relationships in mesenchymal stem cell- and chondrocyte-seeded hydrogels. Tissue Eng Part A **15,** 1041, 2008.
19. Mauck, R.L., Yuan, X., and Tuan, R.S. Chondrogenic differentiation and functional maturation of bovine mesenchymal stem cells in long-term agarose culture. Osteoarthritis Cartilage **14,** 179, 2006.
20. Ahsan, T., and Sah, R.L. Biomechanics of integrative cartilage repair. Osteoarthritis Cartilage **7,** 29, 1999.
21. Wang, Y., Ding, C., Wluka, A.E., Davis, S., Ebeling, P.R., Jones, G., and Cicuttini, F.M. Factors affecting progression of knee cartilage defects in normal subjects over 2 years. Rheumatology **45,** 79, 2006.
22. Fisher, M.B., Henning, E.A., Soegaard, N.B., Dodge, G.R., Steinberg, D.R., and Mauck, R.L. Maximizing cartilage formation and integration via a trajectory-based tissue engineering approach. Biomaterials **35,** 2140, 2014.
23. Irrechukwu, O.N., Lin, P.C., Fritton, K., Doty, S., Pleshko, N., and Spencer, R.G. Magnetic resonance studies of macromolecular content in engineered cartilage treated with pulsed low-intensity ultrasound. Tissue Eng Part A **17,** 407, 2011.
24. Muller, B., Beckmann, F., Huser, M., Maspero, F., Szekely, G., Ruffieux, K., Thurner, P., and Wintermantel, E. Non-destructive three-dimensional evaluation of a polymer sponge by micro-tomography using synchrotron radiation. Biomol Eng **19,** 73, 2002.
25. Xuan, J.W., Bygrave, M., Jiang, H.Y., Valiyeva, F., Dunmore-Buyze, J., Holdsworth, D.W., Izawa, J.I., Bauman, G., Moussa, M., Winter, S.F., Greenberg, N.M., Chin, J.L., Drangova, M., Fenster, A., and Lacefield, J.C. Functional neoangiogenesis imaging of genetically engineered mouse prostate cancer using three-dimensional power Doppler ultrasound. Cancer Res **67,** 2830, 2007.
26. Georgakoudi, I., Rice, W.L., Hronik-Tupaj, M., and Kaplan, D.L. Optical spectroscopy and imaging for the noninvasive evaluation of engineered tissues. Tissue Eng Part B Rev **14,** 321, 2008.
27. Reiter, D.A., Irrechukwu, O., Lin, P.C., Moghadam, S., Von Thaer, S., Pleshko, N., and Spencer, R.G. Improved MR-based characterization of engineered cartilage using multiexponential T-2 relaxation and multivariate analysis. NMR Biomed **25,** 476, 2012.
28. Kotecha, M., Klatt, D., and Magin, R.L. Monitoring cartilage tissue engineering using magnetic resonance spectroscopy, imaging, and elastography. Tissue Eng Part B Rev **19,** 470, 2013.
29. Kotecha, M., Ravindran, S., Schmid, T.M., Vaidyanathan, A., George, A., and Magin, R.L. Application of sodium triple-quantum coherence NMR spectroscopy for the study of growth dynamics in cartilage tissue engineering. NMR Biomed **26,** 709, 2013.
30. Majumdar, S., Pothirajan, P., Dorcemus, D., Nukavarapu, S., and Kotecha, M. High field sodium MRI assessment of stem cell chondrogenesis in a tissue-engineered matrix. Ann Biomed Eng **44,** 1120, 2016.
31. Miyata, S., Homma, K., Numano, T., Tateishi, T., and Ushida, T. Evaluation of negative fixed-charge density in tissue-engineered cartilage by quantitative MRI and relationship with biomechanical properties. J Biomech Eng Trans ASME **132,** 6, 2010.
32. Miyata, S., Numano, T., Tateishic, T., and Ushida, T. Feasibility of noninvasive evaluation of biophysical properties of tissue-engineered cartilage by using quantitative MRI. J Biomech **40,** 2990, 2007.
33. Ramaswamy, S., Greco, J.B., Uluer, M.C., Zhang, Z.J., Zhang, Z.L., Fishbein, K.W., and Spencer, R.G. Magnetic resonance imaging of chondrocytes labeled with superparamagnetic iron oxide nanoparticles in tissue-engineered cartilage. Tissue Eng Part A **15,** 3899, 2009.
34. Ramaswamy, S., Uluer, M.C., Leen, S., Bajaj, P., Fishbein, K.W., and Spencer, R.G. Noninvasive assessment of glycosaminoglycan production in injectable tissue-engineered cartilage constructs using magnetic resonance imaging. Tissue Eng Part C Methods **14,** 243, 2008.
35. Schulz, R., Hohle, S., Zernia, G., Zscharnack, M., Schiller, J., Bader, A., Arnold, K., and Huster, D. Analysis of extracellular matrix production in artificial cartilage constructs by histology, imunocytochemistry, mass spectrometry, and NMR spectroscopy. J Nanosci Nanotechnol **6,** 2368, 2006.
36. Xu, H.H., Othman, S.F., and Magin, R.L. Monitoring tissue engineering using magnetic resonance imaging. J Biosci Bioeng **106,** 515, 2008.

37. Mansour, J.M., Lee, Z.H., and Welter, J.F. Nondestructive techniques to evaluate the characteristics and development of engineered cartilage. Ann Biomed Eng **44,** 733, 2016.
38. Siebelt, M., Groen, H.C., Koelewijn, S.J., de Blois, E., Sandker, M., Waarsing, J.H., Mueller, C., van Osch, G., de Jong, M., and Weinans, H. Increased physical activity severely induces osteoarthritic changes in knee joints with papain induced sulfate-glycosaminoglycan depleted cartilage. Arthritis Res Ther **16,** 12, 2014.
39. Boskey, A., and Camacho, N.P. FT-IR imaging of native and tissue-engineered bone and cartilage. Biomaterials **28,** 2465, 2007.
40. McGoverin, C.M., Hanifi, A., Palukuru, U.P., Yousefi, F., Glenn, P.B.M., Shockley, M., Spencer, R.G., and Pleshko, N. Nondestructive assessment of engineered cartilage composition by near infrared spectroscopy. Ann Biomed Eng **44,** 680, 2016.
41. Siesler, H.W., Ozaki, Y., Kawata, S., and Heise, H.M. Near-Infrared Spectroscopy: Principles, Instruments, Applications. Weinheim, Germany: John Wiley & Sons, 2008.
42. Afara, I., Prasadam, I., Crawford, R., Xiao, Y., and Oloyede, A. Non-destructive evaluation of articular cartilage defects using near-infrared (NIR) spectroscopy in osteoarthritic rat models and its direct relation to Mankin score. Osteoarthritis Cartilage **20,** 1367, 2012.
43. Hanifi, A., Bi, X.H., Yang, X., Kavukcuoglu, B., Lin, P.C., DiCarlo, E., Spencer, R.G., Bostrom, M.P.G., and Pleshko, N. Infrared fiber optic probe evaluation of degenerative cartilage correlates to histological grading. Am J Sports Med **40,** 2853, 2012.
44. Hanh, B.D., Neubert, R.H.H., Wartewig, S., Christ, A., and Hentzsch, C. Drug penetration as studied by noninvasive methods: Fourier transform infrared-attenuated total reflection, Fourier transform infrared, and ultraviolet photoacoustic spectroscopy. J Pharm Sci **89,** 1106, 2000.
45. Bursac, P.M., Freed, L.E., Biron, R.J., and Vunjak-Novakovic, G. Mass transfer studies of tissue engineered cartilage. Tissue Eng **2,** 141, 1996.
46. Afara, I., Singh, S., and Oloyede, A. Application of near infrared (NIR) spectroscopy for determining the thickness of articular cartilage. Med Eng Phys **35,** 88, 2013.
47. Padalkar, M.V., and Pleshko, N. Wavelength-dependent penetration depth of near infrared radiation into cartilage. Analyst **140,** 2093, 2015.
48. Palukuru, U.P., McGoverin, C.M., and Pleshko, N. Assessment of hyaline cartilage matrix composition using near infrared spectroscopy. Matrix Biol **38,** 3, 2014.
49. Kim, I.L., Mauck, R.L., and Burdick, J.A. Hydrogel design for cartilage tissue engineering: a case study with hyaluronic acid. Biomaterials **32,** 8771, 2011.
50. Burdick, J.A., Chung, C., Jia, X., Randolph, M.A., and Langer, R. Controlled degradation and mechanical behavior of photopolymerized hyaluronic acid networks. Biomacromolecules **6,** 386, 2005.
51. Huang, A.H., Yeger-McKeever, M., Stein, A., and Mauck, R.L. Tensile properties of engineered cartilage formed from chondrocyte-and MSC-laden hydrogels. Osteoarthritis Cartilage **16,** 1074, 2008.
52. Rinnan, Ã.S., van den Berg, F., and Engelsen, S.R.B. Review of the most common pre-processing techniques for near-infrared spectra. TrAC Trends Anal Chem **28,** 1201, 2009.
53. Rieppo, L., Saarakkala, S., Nãrhi, T., Helminen, H.J., Jurvelin, J.S., and Rieppo, J. Application of second derivative spectroscopy for increasing molecular specificity of Fourier transform infrared spectroscopic imaging of articular cartilage. Osteoarthritis Cartilage **20,** 451, 2012.
54. Esbensen, K.H., Guyot, D., Westad, F., and Houmoller, L.P. Multivariate Data Analysis-In Practice: An Introduction to Multivariate Data Analysis and Experimental Design. Oslo, Norway: CAMO Process AS, 2002.
55. Mauck, R.L., Soltz, M.A., Wang, C.C.B., Wong, D.D., Chao, P.-H.G., Valhmu, W.B., Hung, C.T., and Ateshian, G.A. Functional tissue engineering of articular cartilage through dynamic loading of chondrocyte-seeded agarose gels. J Biomech Eng **122,** 252, 2000.
56. Park, S., Nicoll, S.B., Mauck, R.L., and Ateshian, G.A. Cartilage mechanical response under dynamic compression at physiological stress levels following collagenase digestion. Ann Biomed Eng **36,** 425, 2008.
57. Farndale, R.W., Buttle, D.J., and Barrett, A.J. Improved quantitation and discrimination of sulphated glycosaminoglycans by use of dimethylmethylene blue. Biochim Biophys Acta **883,** 173, 1986.
58. Hoemann, C.D., Sun, J., Chrzanowski, V., and Buschmann, M.D. A multivalent assay to detect glycosaminoglycan, protein, collagen, RNA, and DNA content in milligram samples of cartilage or hydrogel-based repair cartilage. Anal Biochem **300,** 1, 2002.
59. Luck, W.A.P. Structure of Water and Aqueous Solutions. Weinheim, Germany: Verlag Chemie, 1974.
60. Burns, D.A., and Ciurczak, E.W. Handbook of near-infrared analysis. New York, NY: CRC Press, 2007.
61. Hunter, C.J., and Levenston, M.E. Maturation and integration of tissue-engineered cartilages within an in vitro defect repair model. Tissue Eng **10,** 736, 2004.
62. Bian, L.M., Fong, J.V., Lima, E.G., Stoker, A.M., Ateshian, G.A., Cook, J.L., and Hung, C.T. Dynamic mechanical loading enhances functional properties of tissue-engineered cartilage using mature canine chondrocytes. Tissue Eng Part A **16,** 1781, 2010.
63. Kim, M., Erickson, I.E., Choudhury, M., Pleshko, N., and Mauck, R.L. Transient exposure to TGF-beta 3 improves the functional chondrogenesis of MSC-laden hyaluronic acid hydrogels. J Mech Behav Biomed Mater **11,** 92, 2012.
64. Chung, C., Beecham, M., Mauck, R.L., and Burdick, J.A. The influence of degradation characteristics of hyaluronic acid hydrogels on in vitro neocartilage formation by mesenchymal stem cells. Biomaterials **30,** 4287, 2009.
65. Isogai, N., Kusuhara, H., Ikada, Y., Ohtani, H., Jacquet, R., Hillyer, J., Lowder, E., and Landis, W.J. Comparison of different chondrocytes for use in tissue engineering of cartilage model structures. Tissue Eng **12,** 691, 2006.
66. Miot, S., Brehm, W., Dickinson, S., Sims, T., Wixmerten, A., Longinotti, C., Hollander, A.P., Mainil-Varlet, P., and Martin, I. Influence of in vitro maturation of engineered cartilage on the outcome of osteochondral repair in a goat model. Eur Cells Mater **23,** 222, 2012.
67. Vinardell, T., Thorpe, S.D., Buckley, C.T., and Kelly, D.J. Chondrogenesis and integration of mesenchymal stem cells within an in vitro cartilage defect repair model. Ann Biomed Eng **37,** 2556, 2009.
68. Obradovic, B., Martin, I., Padera, R.F., Treppo, S., Freed, L.E., and Vunjak-Novakovic, G. Integration of engineered cartilage. J Orthop Res **19,** 1089, 2001.
69. Spaln, G., Plettenberg, H., Nagel, H., Kahl, E., Klinger, H.M., Muckley, T., Gunther, M., Hofmann, G.O., and Mollenhauer, J.A. Evaluation of cartilage defects with near-

infrared spectroscopy (NIR): an ex vivo study. Med Eng Phys **30,** 285, 2008.
70. Afara, I.O., Prasadam, I., Moody, H., Crawford, R., Xiao, Y., and Oloyede, A. Near infrared spectroscopy for rapid determination of mankin score components: a potential tool for quantitative characterization of articular cartilage at surgery. Arthroscopy **30,** 1146, 2014.
71. Afara, I.O., Moody, H., Singh, S., Prasadam, I., and Oloyede, A. Spatial mapping of proteoglycan content in articular cartilage using near-infrared (NIR) spectroscopy. Biomed Opt Express **6,** 144, 2015.
72. Hanifi, A., Palukuru, U., McGoverin, C., Shockley, M., Frank, E., Grodzinsky, A., Spencer, R.G., and Pleshko, N. Near infrared spectroscopic assessment of developing engineered tissues: correlations with compositional and mechanical properties. Analyst **142,** 1320, 2017.
73. Spahn, G., Klinger, H.M., Baums, M., Hoffmann, M., Plettenberg, H., Kroker, A., and Hofmann, G.O. Near-infrared spectroscopy for arthroscopic evaluation of cartilage lesions results of a blinded, prospective, interobserver study. Am J Sports Med **38,** 2516, 2010.
74. Spahn, G., Plettenberg, H., Kahl, E., Klinger, H.M., Muckley, T., and Hofmann, G.O. Near-infrared (NIR) spectroscopy. A new method for arthroscopic evaluation of low grade degenerated cartilage lesions. Results of a pilot study. BMC Musculoskelet Disord **8,** 9, 2007.
75. McGoverin, C.M., Lewis, K., Yang, X., Bostrom, M.P.G., and Pleshko, N. The contribution of bone and cartilage to the near-infrared spectrum of osteochondral tissue. Appl Spectrosc **68,** 1168, 2014.
76. Neumann, A.J., Quinn, T., and Bryant, S.J. Nondestructive evaluation of a new hydrolytically degradable and photoclickable PEG hydrogel for cartilage tissue engineering. Acta Biomater **39,** 1, 2016.
77. Trachtenberg, J.E., Vo, T.N., and Mikos, A.G. Pre-clinical characterization of tissue engineering constructs for bone and cartilage regeneration. Ann Biomed Eng **43,** 681, 2015.
78. Kunstar, A., Leferink, A.M., Okagbare, P.I., Morris, M.D., Roessler, B.J., Otto, C., Karperien, M., Van Blitterswijk, C.A., Moroni, L., and van Apeldoorn, A.A. Label-free Raman monitoring of extracellular matrix formation in three-dimensional polymeric scaffolds. J R Soc Interface **10,** 12, 2013.
79. Halliwell, B. Oxidative stress in cell culture: an underappreciated problem? FEBS Lett **540,** 3, 2003.

Address correspondence to:
Nancy Pleshko, PhD
Department of Bioengineering
Temple University
1947 N. 12th Street
Philadelphia, PA 19122

E-mail: npleshko@temple.edu

Received: January 17, 2017
Accepted: April 3, 2017
Online Publication Date: May 15, 2017